

SUPPORTING INFORMATION

Chiral Nanostructures Derived from Europium (III) Complexes for Enhanced Circularly Polarised Luminescence and Antibacterial Activity

Betsy Marydasan,^{a,b} Karthika Suryaaletha,^c Amrutha Manoj Lena,^a Alida Sachin,^a Tsuyoshi Kawai,^d Sabu Thomas^c and Jatish Kumar^{a*}

^a*Department of Chemistry, Indian Institute of Science Education and Research (IISER) Tirupati, Tirupati 517507, India.*

^b*Department of Chemistry, Government Arts College, Thiruvananthapuram, Kerala – 695014, India*

^c*Cholera and Biofilm Research laboratory, Rajiv Gandhi Centre for Biotechnology (National Institute under the Dept. of Biotechnology, Govt. of India), Trivandrum, Kerala, India.*

^d*Graduate School of Materials Science, Nara Institute of Science and Technology, Ikoma, Nara 630-0192, Japan.*

Email: jatish@iisertirupati.ac.in

Page No.	Contents
S3	Fig. S1. Synthetic scheme for the preparation of the complexes
S3	Table S1: XRD data of the complex
S3	Fig. S2. Single crystal XRD of Cs ⁺ [Eu((+)-tfac) ₄] ⁻ complex
S4	Fig. S3. CD, UV-vis, CPL and PL spectra of complexes in chloroform
S4	Fig. S4. CD, UV-vis, CPL and PL spectra of Eu((+)-tfac) ₃
S5	Fig. S5. Concentration dependent CPL spectra of Cs complex in chloroform
S5	Table S2. g _{lum} values of Cs complex in chloroform at different concentrations
S5	Fig. S6. Lifetime plots of complexes in chloroform
S6	Fig. S7. CD and UV-vis spectra of complexes in PMMA film
S6	Fig. S8. CD, UV-vis and lifetime plots of complexes in PMMA film

S7	Fig. S9. Concentration dependent CPL spectra of Cs complex in PMMA films
S7	Table S3. g_{lum} values of Cs complex in PMMA films at different concentrations
S8	Fig. S10. CD spectra of the Cs derivative from different points on the film.
S8	Fig. S11. CPL spectra of the Cs derivative from different points on the film.
S8	Table S4. g_{lum} values from different points on the PMMA films
S9	Fig. S12. Photographic images of complexes under UV light
S9	Fig. S13. SEM images of nanostructures formed in DMSO
S10	Fig. S14. Concentration dependent CPL spectra of Cs complex in DMSO
S10	Table S5. g_{lum} values of Cs complex in DMSO at different concentrations
S11	Fig. S15. CPL and PL spectra of the complexes in DMSO:water mixture
S12	Fig. S16. Percentage inhibition of $Rb^+[Eu(tfac)_4]^-$ against major pathogens.
S12	Fig. S17. Percentage inhibition of $K^+[Eu(tfac)_4]^-$ against major pathogens.

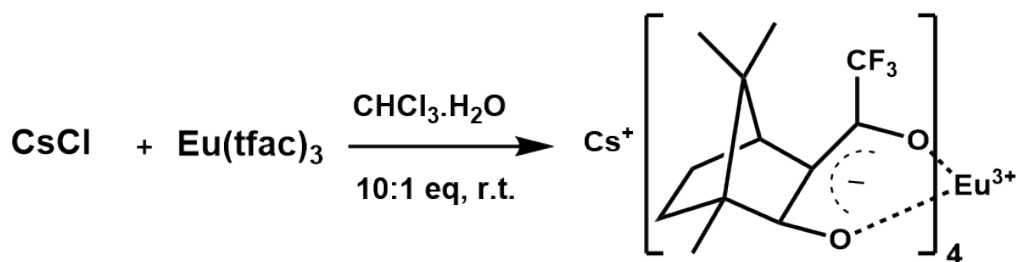


Figure S1. Synthetic scheme adopted the preparation of the Eu complex, $\text{Cs}^+[\text{Eu}((+)\text{-tfac})_4]^-$. Similar synthetic protocols were adopted for other complexes (Na, K and Rb) using the respective metal salts (Na_2SO_4 , KCl and RbCl).

Table S1. Structural refinement and crystal data of $\text{Cs}^+[\text{Eu}((+)\text{-tfac})_4]^-$

Empirical formula	$\text{C}_{48}\text{H}_{56}\text{CsEuF}_{12}$	μ (Mo $K\alpha$)/ cm^{-1}	20.315 cm^{-1}
Formula weight	1305.81	measured reflections	21982
Crystal system	Tetragonal	unique reflections	2909
Space group	I4 (#79)	Reflection/Parameter Ratio	17.21
$a/\text{Å}$	17.4004(3)	Residuals: R1	0.0260
$c/\text{Å}$	8.41371(15)	Residuals: Rw	0.0727
Z	2	goodness of fitting	1.191
$V/(\text{Å}^3)$	2547.45(8)	T/K	123

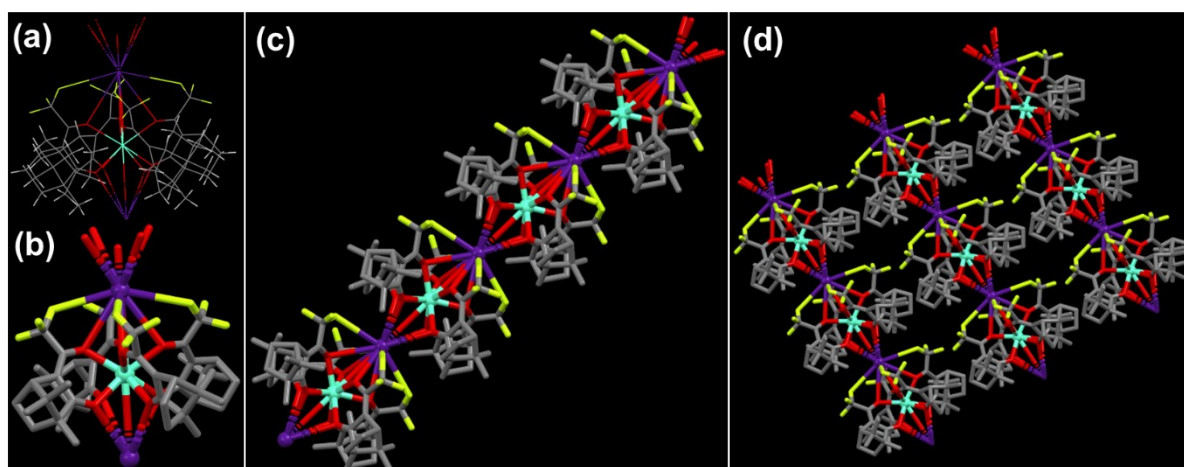


Figure S2. (a-c) X-ray crystal structure of (a,b) $\text{Cs}^+[\text{Eu}((+)\text{-tfac})_4]^-$ complex, (c) its one-dimensional array and (d) the network structures.

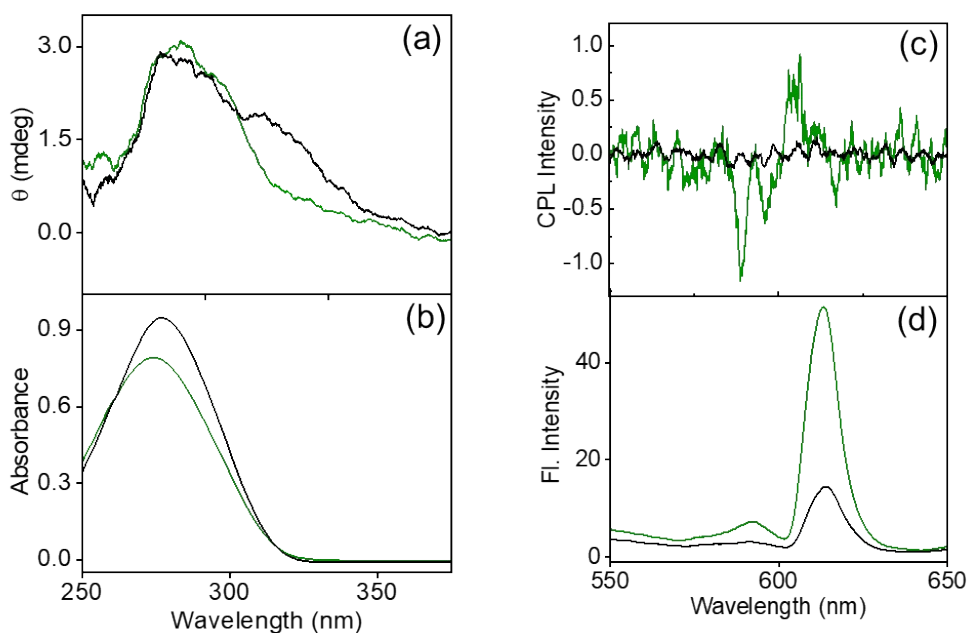


Figure S3. (a) CD, (b) absorption, (c) CPL and (d) luminescence spectra of $\text{K}^+[\text{Eu}(\text{tfac})_4]^-$ (green traces) and $\text{Na}^+[\text{Eu}(\text{tfac})_4]^-$ (black traces) in chloroform (concentration = 2.0 mM; excitation wavelength $\lambda_{\text{ex}} = 317$ nm).

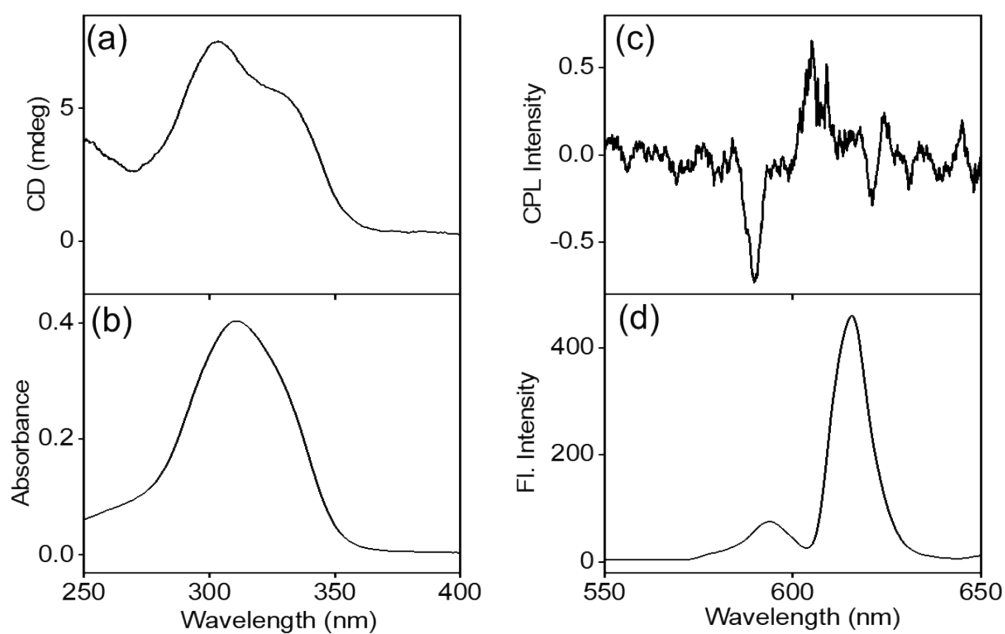


Figure S4. (a) CD, (b) absorption, (c) CPL and (d) luminescence spectra of $\text{Eu}(++)\text{-tfac}_3$ in chloroform (concentration = 2.0 mM; excitation wavelength $\lambda_{\text{ex}} = 352$ nm).

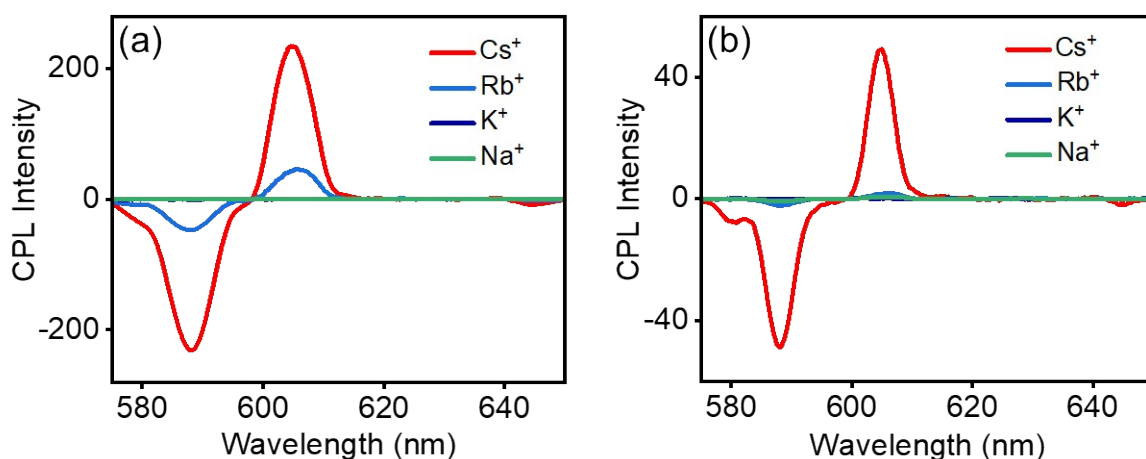


Figure S5. CPL spectra of (a) 2.0 mM and (b) 1.0 mM solution of the $M^+[Eu(tfac)_4]^-$ complexes ($M = Cs, Rb, K, Na$) in chloroform.

Table S2. The g_{lum} values of 2.0 mM and 1.0 mM solution the complexes in chloroform.

Chloroform (2.0 mM)			Chloroform (1.0 mM)		
M	$g_{lum} (^5D_0 - ^7F_1)$	$g_{lum} (^5D_0 - ^7F_2)$	M	$g_{lum} (^5D_0 - ^7F_1)$	$g_{lum} (^5D_0 - ^7F_2)$
Cs	-0.701	0.128	Cs	-0.513	0.046
Rb	-0.155	0.051	Rb	-0.145	0.047
K	-0.025	0.003	K	-0.020	0.025
Na	-0.005	0.001	Na	-0.001	0.002

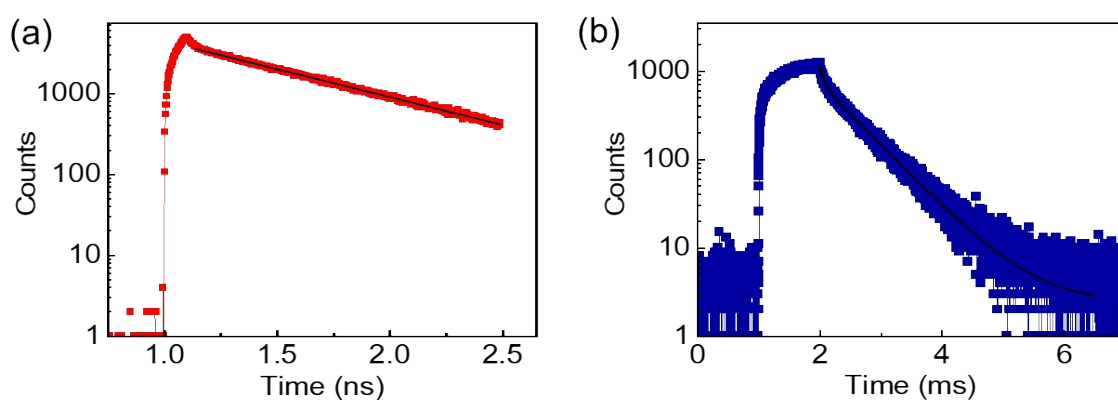


Figure S6. (a) Luminescence lifetime plots of (a) $Cs^+[Eu((+)-tfac)_4]^-$ and (d) $Rb^+[Eu((+)-tfac)_4]^-$ in chloroform.

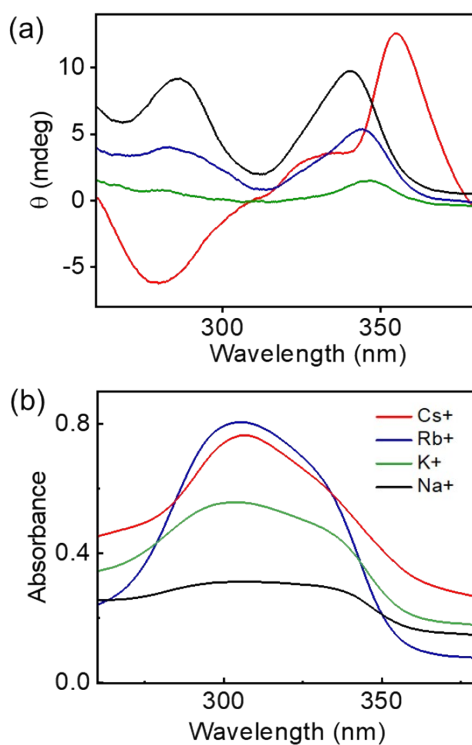


Figure S7. Solid state (a) CD and (b) absorption spectra of PMMA films of the $M^+[Eu(tfac)_4]^-$ complexes.

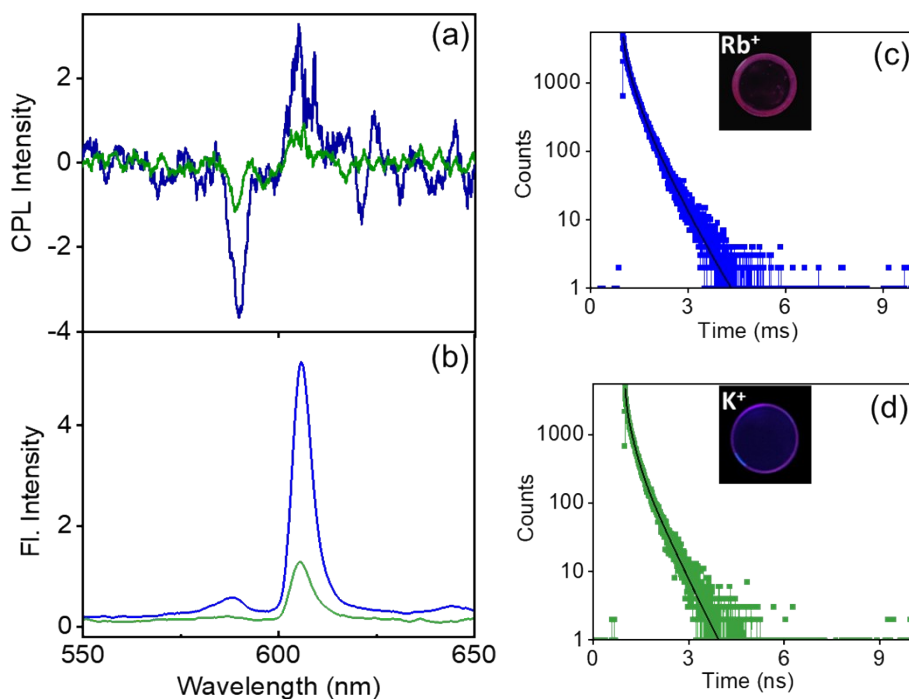


Figure S8. (a) CPL and (b) Fluorescence spectra of the $Rb^+[Eu((+)-tfac)_4]^-$ (blue traces) and $K^+[Eu((+)-tfac)_4]^-$ (green traces) embedded in the PMMA films. The luminescence lifetime plots of the PMMA films composed of (c) $Rb^+[Eu((+)-tfac)_4]^-$ and (d) $K^+[Eu((+)-tfac)_4]^-$.

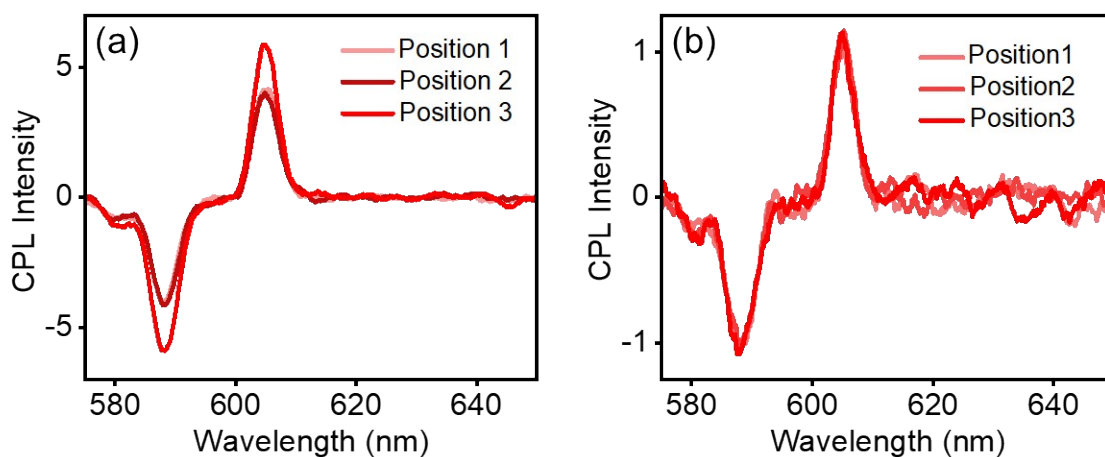


Figure S9. CPL spectra of $\text{Cs}^+[\text{Eu}((+)\text{-tfac})_4]^-$ collected from different points on the PMMA film prepared using a (a) 2.0 mM and (b) 1.0 mM solution of the complex in chloroform. Position 3 refers to the spectra collected after flipping the film.

Table S3. The g_{lum} values collected from different points on the PMMA films of $\text{Cs}^+[\text{Eu}(\text{tfac})_4]^-$ complexes prepared using 2.0 mM and 1.0 mM solution in chloroform.

	PMMA (2.0 mM)		PMMA (1.0 mM)	
	$g_{\text{lum}@595}$	$g_{\text{lum}@610}$	$g_{\text{lum}@595}$	$g_{\text{lum}@610}$
Position 1	-0.290	0.031	-0.071	0.007
Position 2	-0.289	0.029	-0.070	0.007
Position 3	-0.280	0.028	-0.072	0.007

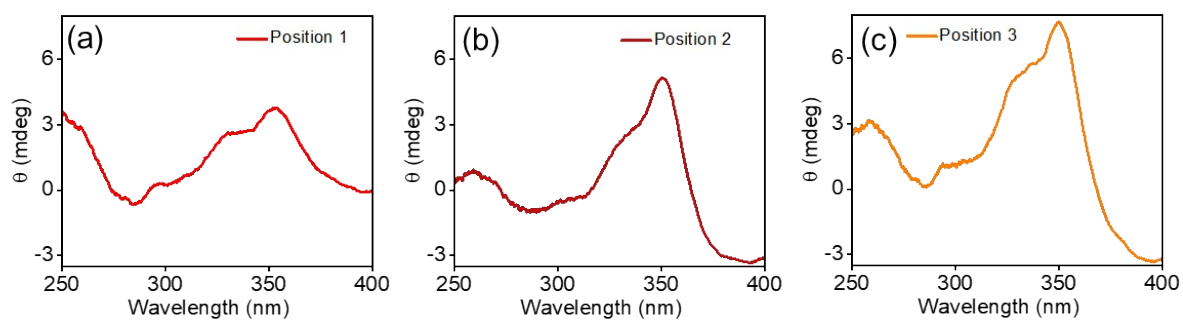


Figure S10. CD spectra of $\text{Cs}^+[\text{Eu}((+)\text{-tfac})_4]^-$ collected from different points after rotation and flipping of the PMMA film. Position 3 refers to spectra collected after flipping the film.

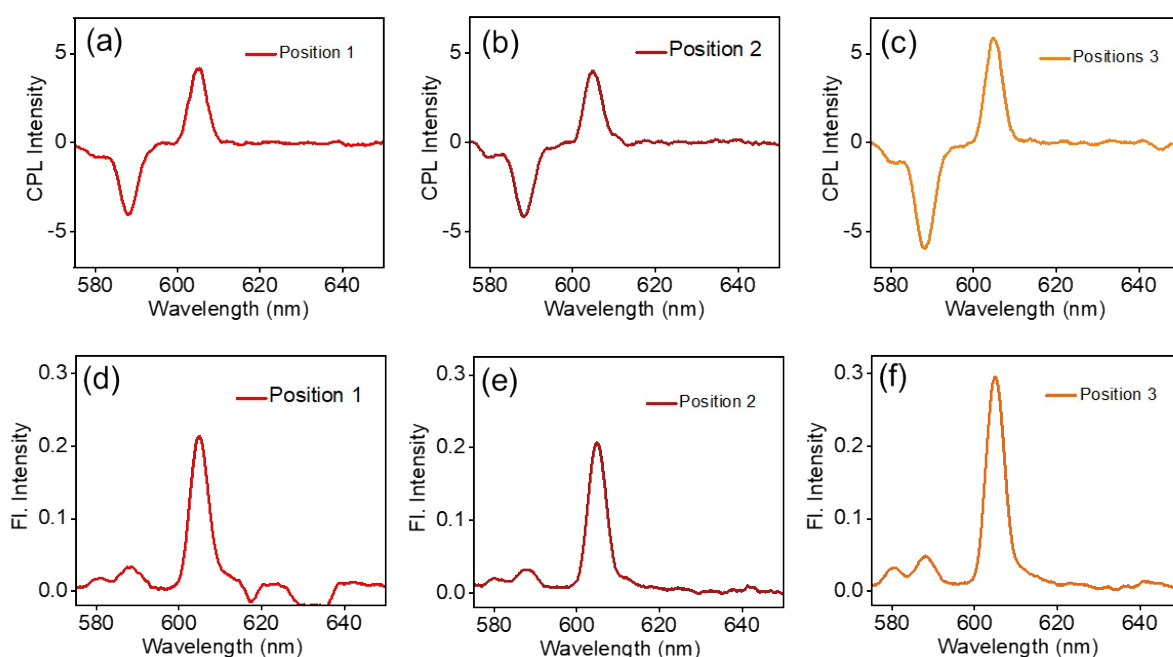


Figure S11. (a-c) CPL and (d-f) luminescence spectra of $\text{Cs}^+[\text{Eu}((+)\text{-tfac})_4]^-$ collected from different points after rotation and flipping of the PMMA film. Position 3 refers to the spectra collected after flipping the film.

Table S4. Chiral anisotropy values of $\text{Cs}^+[\text{Eu}((+)\text{-tfac})_4]^-$ PMMA film collected from different points on the film.

	$g_{\text{lum}@595}$	$g_{\text{lum}@610}$
Position 1	-0.290	0.031
Position 2	-0.289	0.029
Position 3	-0.280	0.028

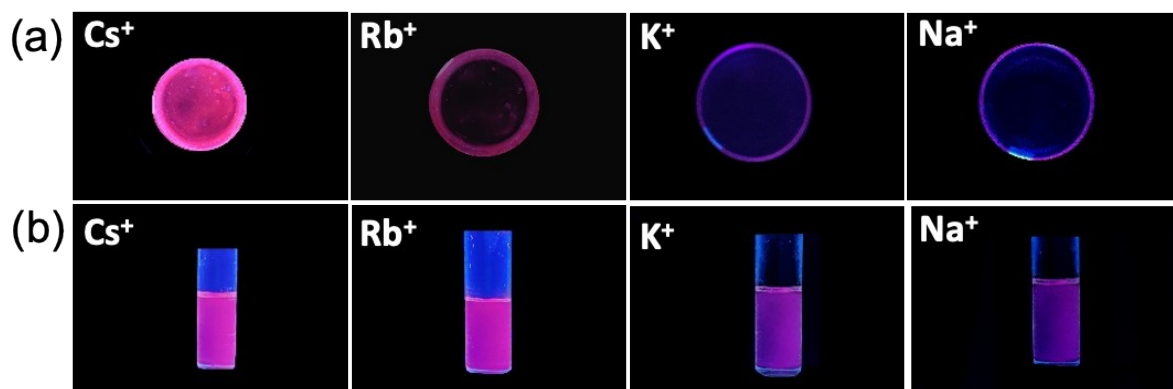


Figure S12. Photographic images of (a) solid films and (b) solution samples of $M^+[Eu((+)-tfac)_4]^-$ ($M = Cs, Rb, K, Na$) complexes in DMSO taken under 365 nm UV light.

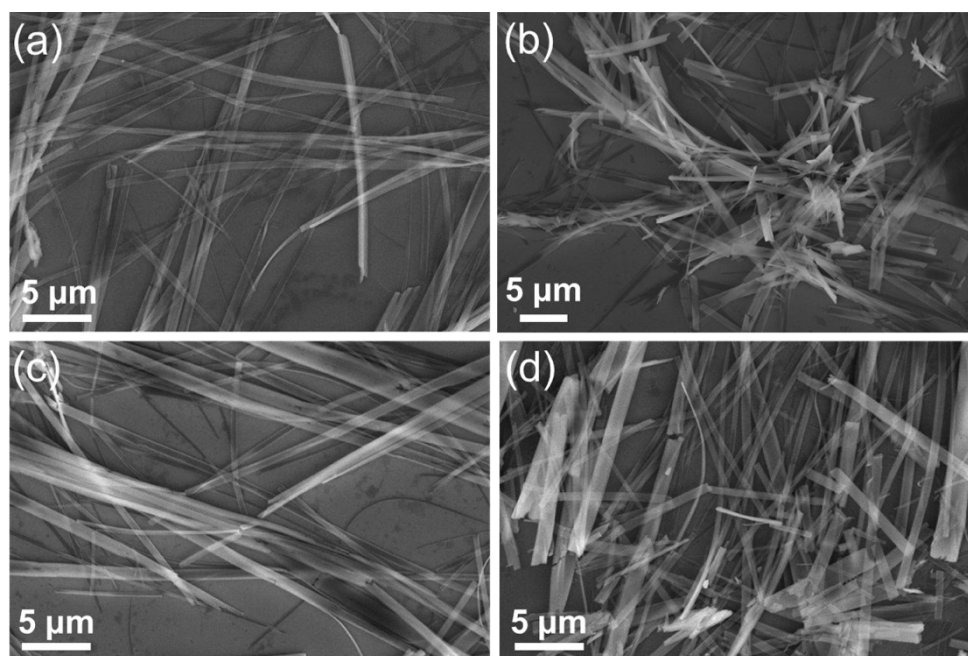


Figure S13. SEM images of nanostructures formed in DMSO solutions of (a) $Cs^+[Eu((+)-tfac)_4]^-$, (b) $Rb^+[Eu((+)-tfac)_4]^-$, $K^+[Eu((+)-tfac)_4]^-$ and $Na^+[Eu((+)-tfac)_4]^-$.

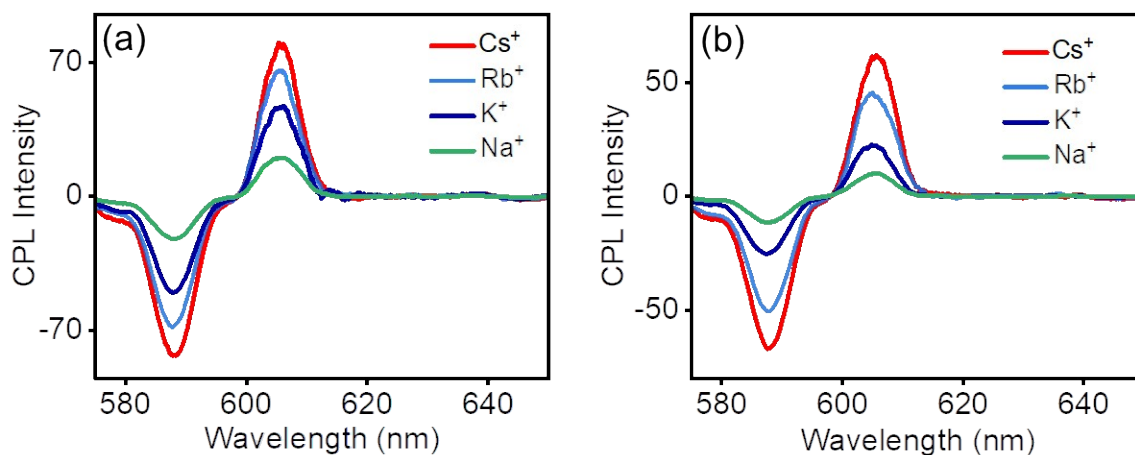


Figure S14. CPL spectra of (a) 2.0 mM and (b) 1.0 mM solution of the $M^+[Eu(tfac)_4]^-$ complexes ($M = Cs, Rb, K, Na$) in DMSO.

Table S5. The g_{lum} values of 2.0 mM and 1.0 mM solution the complexes in DMSO.

DMSO (2.0 mM)			DMSO (1.0 mM)		
M	$g_{lum} (^5D_0 - ^7F_1)$	$g_{lum} (^5D_0 - ^7F_2)$	M	$g_{lum} (^5D_0 - ^7F_1)$	$g_{lum} (^5D_0 - ^7F_2)$
Cs	-0.691	0.133	Cs	-0.518	-0.054
Rb	-0.565	0.054	Rb	-0.483	-0.047
K	-0.492	0.047	K	-0.465	-0.042
Na	-0.440	0.041	Na	-0.256	-0.024

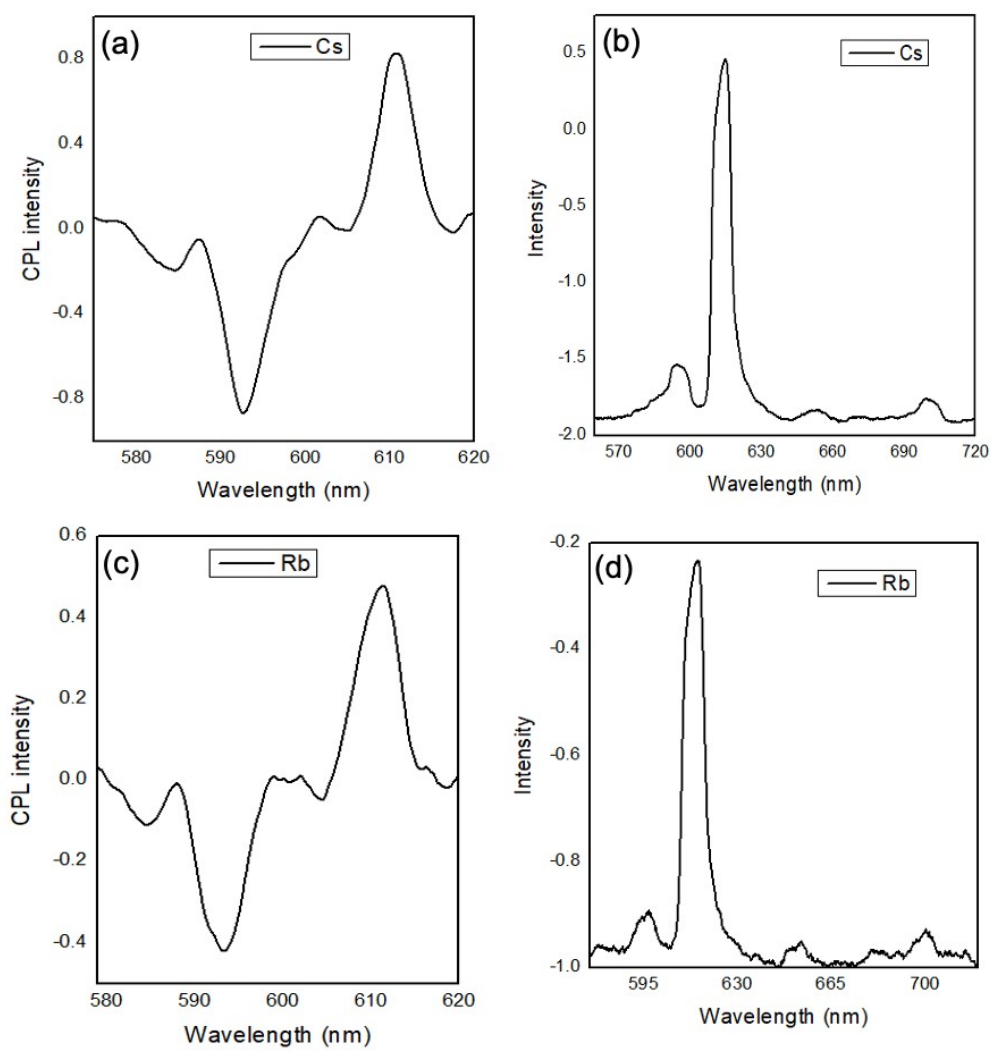


Figure S15. (a,c) CPL and (b,d) fluorescence spectra of (a,b) Cs⁺[Eu((+)-tfac)₄]⁻ and (c,d) Rb⁺[Eu((+)-tfac)₄]⁻ collected in DMSO:water (1:4) mixture.

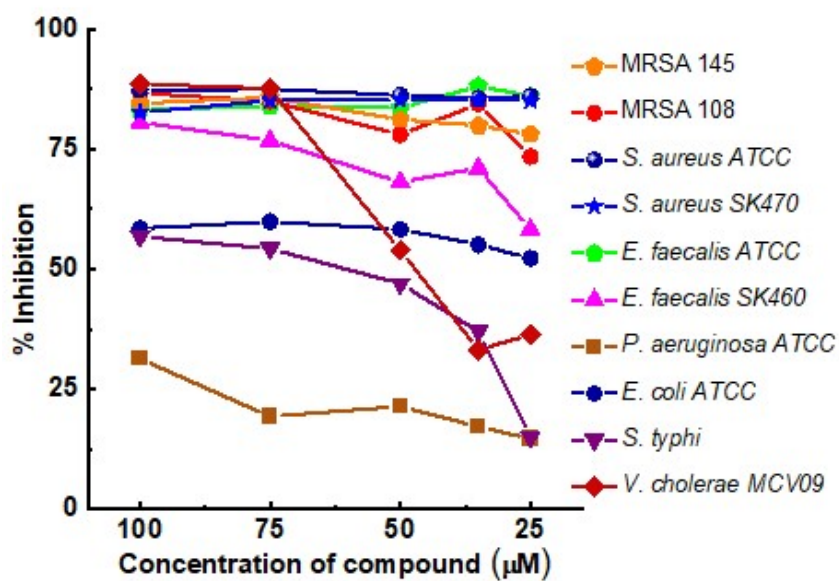


Figure S16. Percentage inhibition of $\text{Rb}^+[\text{Eu}((+)\text{-tfac})_4]^-$ compound against major Gram positive and Gram-negative pathogens.

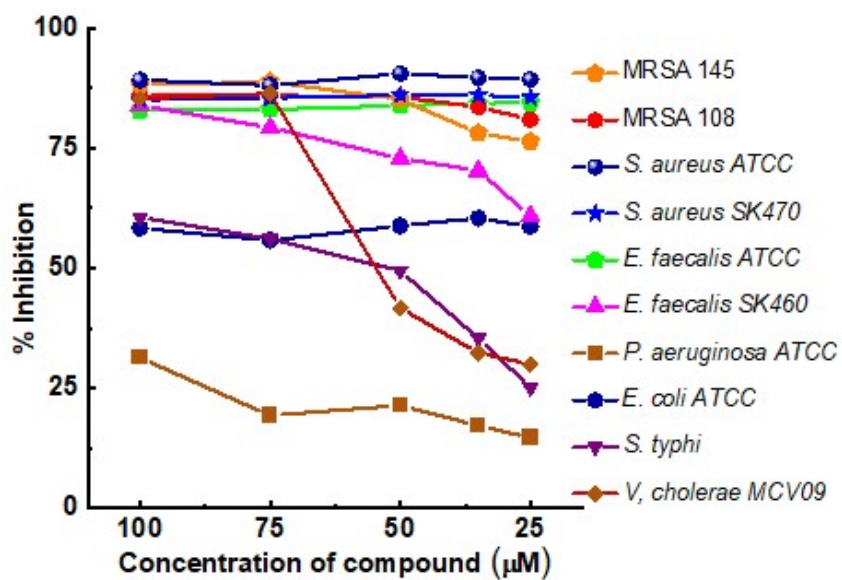


Figure S17. Percentage inhibition of $\text{K}^+[\text{Eu}((+)\text{-tfac})_4]^-$ compound against major Gram positive and Gram-negative pathogens.